SUPPLEMENTAL DATA

Radiochemistry

Quality control testing was performed with a Waters HPLC system (1525 or e2695), monitoring the column effluent with ultraviolet (Waters 2489, λ = 254 nM) and radioactivity (Bioscan FC-200) detectors. The HPLC column was a Phenomenex Kinetex C18 4.6 × 250 mm analytical column, eluting with a mixture of methanol/water/triethylamine (50/50/0.24, to 90/10/0.25 v/v/v over 12 min) at a flow rate of 1 mL/min, and the data were analyzed with Waters Empower software. Radioactivity was measured with a Capintec CRC-25 dose calibrator. Radionuclidic identity was determined by γ spectroscopy using a Canberra 802 multichannel analyzer. pH was measured with indicator strips (range, 0–14; Sigma). Cryptand 222 (Kryptofix-222) content was measured using a TLC test. Residual solvent analysis was performed using a Perkin-Elmer Clarus 500 gas chromatograph fitted with a Restek Stabilwax (30 m × 0.53 mm × 1 μm) column. Pyrogen content was measured with a Charles River Laboratories Endosafe PTS-100. Sterility tests were performed by inoculating a sample of the drug product in fluid thioglycollate medium and trypticase soy broth (Northeast Laboratories) and monitoring for 2 wk, per U.S. Pharmacopeia guidelines.

Animals

All experiments were conducted in accordance with the U.S. Public Health Service's Policy on Humane Care and Use of Laboratory Animals and with institutional approval. Adult rhesus macaques (*Macaca mulatta,* 2 females and 3 males, 7.8 ± 2.9 kg) were studied. Animals were first anesthetized with intramuscular ketamine (10 mg/kg) and given glycopyrrolate (0.1–0.2 mg/kg) to reduce secretions, transferred to the camera, and intubated for continuous anesthesia with ~2.5% isoflurane mixed with oxygen. Radiotracer was injected 2 h after administration of anesthetics to allow for stabilization of the animals' physiology. An intravenous catheter was used for administration of fluids for hydration. Body temperature was maintained by a heated water blanket and monitored with a rectal thermometer. Vital signs including heart rate, respiration rate, blood pressure, oxygen saturation, and body temperature were monitored continuously and recorded every 10–20 min during the study.

Arterial Input Function

After tracer administration, radial artery blood samples were collected every 45 s until 6 min and then at 8, 10, 15, 20, 25, 30, 45, 60, 90, 120, 150, and 180 min. Radioactivity in whole blood and total plasma was measured in all samples using 200-μL aliquots, counted with a γ counter (Wallac 2480 Wizard 3M Automatic; Perkin-Elmer) for 1 min (400- to 1,400-keV energy window). For 6 samples (6, 15, 30, 60, 120, and 180 min), plasma was further processed by acetonitrile denaturation, treating 1 mL of plasma with 1 mL of acetonitrile, and radiometabolites and parent fractions were measured by reverse-phase HPLC performed on a Phenomenex Luna C18(2) (10 × 250 mm, 10 μm) at a flow rate of 4 mL/min, the mobile phase consisting of a mixture of methanol/water with 0.8% of triethylamine in a 70/30 ratio. Plasma protein binding was evaluated in vitro, using a blood sample drawn before tracer injection and spiked with ~15 kBq/mL of ^{18}F-MNI-444 at the time of processing. Plasma free fraction was determined using 200-μL aliquots of plasma pipetted in duplicates into ultrafiltration units (Amicon Centrifree 30; Millipore) and centrifuged at 20°C for 20 min at 3,000*g*. Radioactivity of the ultrafiltrate (50-μL aliquot) and the filtration unit was counted for 1 min (400- to 1,400-keV energy window). The plasma protein binding free fraction (f_p) was calculated as the ratio of the ultrafiltrate activity concentration to the plasma activity concentration. Parent fractions measured for the 6 samples were interpolated to the other sampling times, and the total plasma curve was multiplied by the parent fraction curve to obtain the arterial parent plasma input function used subsequently for the analysis of the PET data. The input function was not corrected for protein binding.

^{18}F-MNI-444 Whole-Body PET Studies

Two adult rhesus monkeys (*Macaca mulatta*), 1 male and 1 female, were used for whole-body PET imaging on a Biograph mCT PET/CT camera (Siemens Healthcare Molecular Imaging) after intravenous bolus injection of ^{18}F-MNI-444 to determine the biodistribution and estimate absorbed radiation doses. Before injection, a CT scan was acquired and used for attenuation and scatter correction. Immediately after radiotracer administration, dynamic 2-dimensional PET scans were acquired from head to thigh over 4 h using 4–5 contiguous 15-cm bed positions and 17–18 frames of increasing duration. Whole-body dynamic PET sinograms were corrected for photon attenuation, scatter, and randoms and reconstructed using the iterative reconstruction method recommended by the camera manufacturer.

Whole-body PET images were imported into PMOD (PMOD Technologies Ltd.,), and volumes of interests (VOIs) were drawn on source organs and around the animal body. Non–decay-corrected time–activity curves were generated and expressed as percentage injected dose (%ID). The residence time τ (ratio of accumulated activity in the source organ [$\bar{A}$] and injected activity [A_0]; $\tau = \bar{A}/A_0$) was calculated as the area under the time–activity curve normalized to %ID from time zero to infinity, assuming only physical decay after the last measurement point. Absorbed radiation dose as well as effective dose (weighted average of the equivalent dose using the tissue weighting factors from ICRP-60) were estimated with OLINDA/EXM 1.0 (Organ Level Internal Dose Assessment) software (*1*) according to the male or female model. Two methods were used for organ and whole-body absorbed dose estimates: the first method assumed that the fractional activity in the monkey organs was similar to humans, and the second method used a residence time scaled to human organ sizes and body weights (*2*,*3*) by multiplying τ by $(b_m/o_m) \times (o_h/b_h)$, where b_m and b_h are the monkey and human body weights, respectively, and o_m and o_h are the monkey and human organ weights, respectively (Supplemental Table 2). Residence times for the small intestine and the upper and lower large intestines were estimated using the International Commission on Radiological Protection, publication 30, gastrointestinal model (*4*) as incorporated in OLINDA/EXM 1.0 (*1*). The fraction of injected activity entering the small intestine was estimated as the highest fraction encountered in the intestinal area within the whole-body scans. To conservatively estimate the absorbed radiation doses, the activity measured in the vertebrae was assumed to be from the red marrow, although a small portion of that activity may have come from the bone. The measured vertebrae τ was multiplied by 100/40 in order to obtain a conservative estimate of whole-body red marrow content, based on previously reported values of red marrow mass in the vertebrae of rhesus monkeys and human subjects (*2*,*5*,*6*).

^{18}F-MNI-444 Dosimetry

^{18}F-MNI-444 whole-body distribution over time is shown in Supplemental Figure 2. The following organs were identified as source organs: brain, heart, liver, gallbladder, intestine, kidneys, urinary bladder, lungs, and vertebrae. Early images showed a notable radioactivity concentration in the heart wall (peak %ID around 2.2% at 5 min after injection), lungs (peak %ID around 5.2% at 2 min after injection), and kidneys (peak %ID around 3.0% at 2 min after

injection). The elimination route of ^{18}F-MNI-444 was via the hepatobiliary and urinary systems, with peak %ID around 2.8% in the gallbladder, 19.5% in the liver, 3.0% in kidneys, and 6.4% (decay-corrected) in the urinary bladder at the end of the imaging period. The calculated absorbed doses and whole-body effective doses obtained using methods 1 and 2 are presented in Supplemental Table 3. Results showed that the organs with the highest absorbed doses were the gallbladder, intestine, liver, and urinary bladder. The average whole-body effective dose was determined to be 0.028 mSv/MBq and 0.022 mSv/MBq for methods 1 and 2, respectively. This radiation exposure is in line with other ^{18}F-labeled tracers (0.019 mSv/MBq for ^{18}F-FDG) and would allow several scans to be performed on the same subject per year with a 180-MBq injected dose.

REFERENCES

1. Stabin MG, Sparks RB, Crowe E. OLINDA/EXM: the second-generation personal computer software for internal dose assessment in nuclear medicine. *J Nucl Med.* 2005;46:1023–1027.

2. Kimura Y, Fujita M, Hong J, et al. Brain and whole-body imaging in rhesus monkeys of ^{11}C-NOP-1A, a promising PET radioligand for nociceptin/orphanin FQ peptide receptors. *J Nucl Med.* 2011;52:1638–1645.

3. Brown AK, Fujita M, Fujimura Y, et al. Radiation dosimetry and biodistribution in monkey and man of ^{11}C-PBR28: a PET radioligand to image inflammation. *J Nucl Med.* 2007;48:2072–2079.

4. Limits for intakes of radionuclides by workers. ICRP publication 30 (part 1). *Ann ICRP.* 1979;2.

5. Cristy M. Active bone marrow distribution as a function of age in humans. *Phys Med Biol.* 1981;26:389–400.

6. Gong JK. Volumetric composition of the monkey skeleton. *Anat Rec.* 1972;172:543–549.

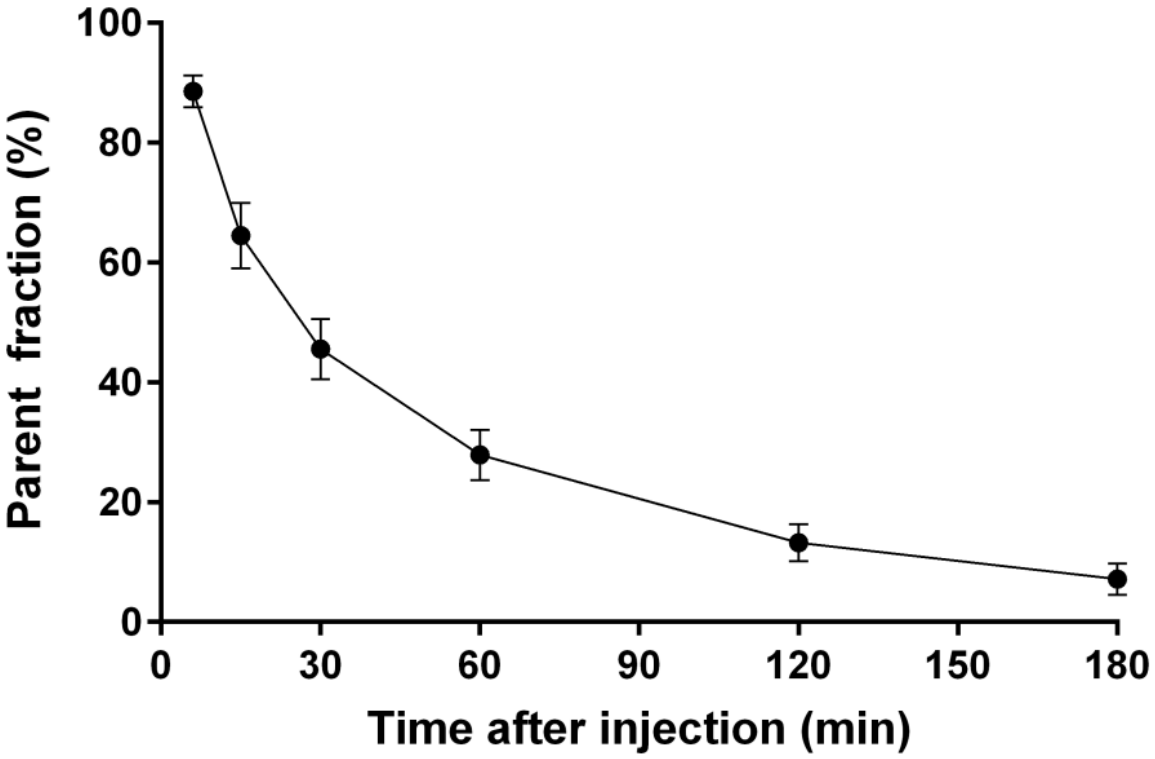

SUPPLEMENTAL FIGURE 1. Average ^{18}F-MNI-444 parent fraction profile in plasma in rhesus macaque (n = 20) after administration. The error bars represent the SD.

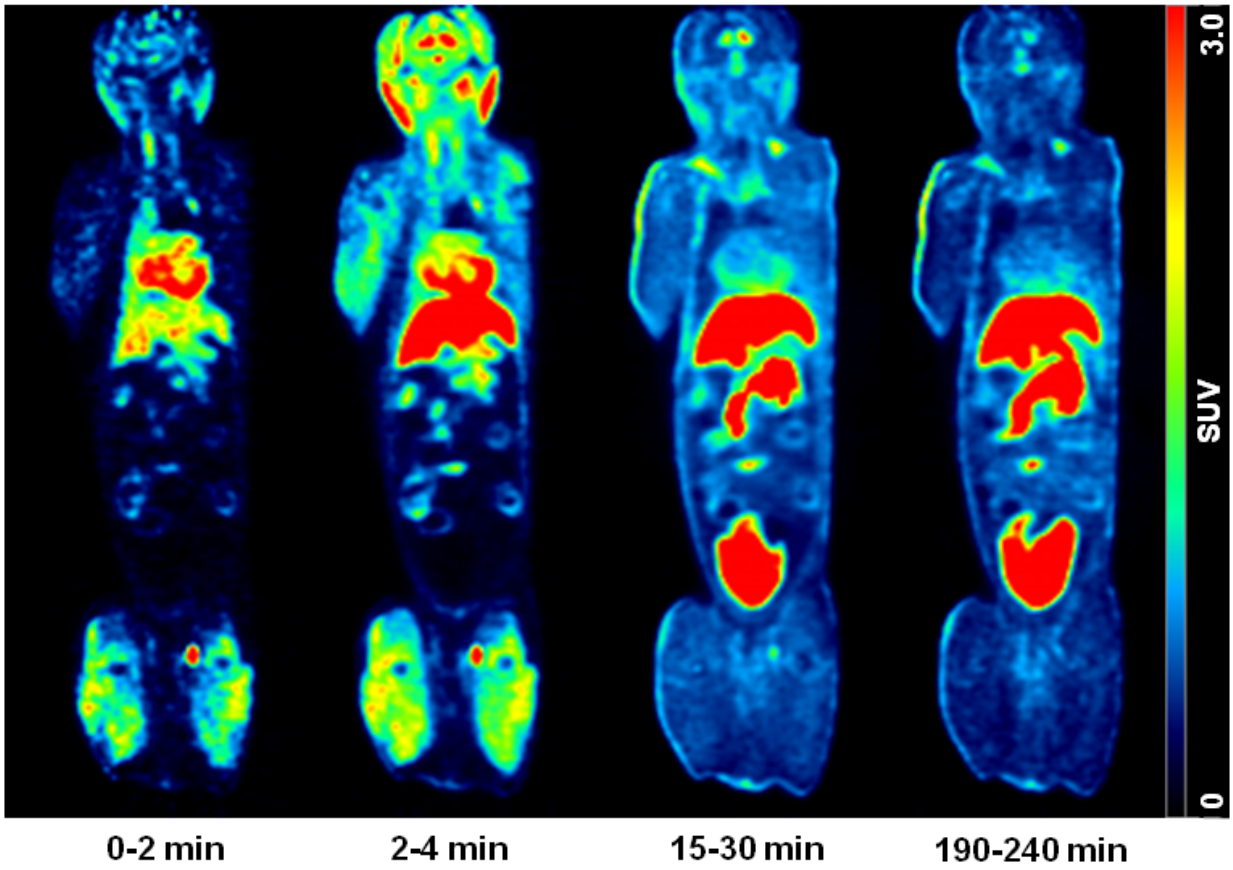

SUPPLEMENTAL FIGURE 2. Whole-body coronal PET images of a male rhesus monkey showing the temporal distribution of ^{18}F-MNI-444 over 4 h after bolus injection of the tracer (images are not corrected for decay).

SUPPLEMENTAL TABLE 1. 18F-MNI-444 VT and BPND Test-retest for LGA, SRTM, and NI-LGA for Acquisitions of 180 and 120 min (n = 2, mean)

Region	180 min of data				120 min of data			
	V_T LGA	BP_{ND} LGA	BP_{ND} SRTM	BP_{ND} NI-LGA	V_T LGA	BP_{ND} LGA	BP_{ND} SRTM	BP_{ND} NI-LGA
Striatum	11.9%	7.1%	8.2%	8.4%	12.7%	8.4%	7.4%	8.5%
Caudate	12.1%	7.7%	10.0%	9.9%	12.8%	8.9%	9.6%	10.2%
Putamen	11.7%	6.6%	6.8%	7.1%	12.4%	7.9%	5.7%	7.2%
Glob. pall.	6.3%	0.6%	4.3%	3.9%	9.3%	4.9%	4.7%	6.1%
Nucl. acc.	10.1%	6.0%	8.7%	8.2%	9.9%	6.1%	8.3%	8.2%
Cerebellum	5.8%	NA	NA	NA	5.2%	NA	NA	NA

LGA = Logan graphical analysis; SRTM = simplified reference tissue model; NI-LGA = noninvasive Logan graphical analysis.

SUPPLEMENTAL TABLE 2. Scaling Factors for Different Organs Determined from Their Percentage Contribution to Total Body Weight for Rhesus Monkeys and Humans

Organ	% total body weight monkey	% total body weight human	Correction factor
Brain	1.4	2	1.41
Heart wall	0.4	1.2	2.60
Liver	2.3	2.5	1.05
Gallbladder	<0.1*	<0.1	0.98
Small intestine	2.3**	0.9	0.39
Upper large intestine	0.5**	0.2	0.39
Lower large intestine	0.5**	0.2	0.39
Gastrointestinal track	3.3	1.3	0.43
Lungs	0.8	1.6	1.96
Kidneys	0.4	0.4	1.09
Urinary bladder†	0.1	0.1	1.00
Remaining	84.9	78.2	0.92

*Gallbladder weight in monkeys was estimated from gallbladder/(liver + gallbladder) in humans since gallbladder + liver was reported for monkeys.

**Relative proportions for small intestine, upper large intestine, and lower large intestine were taken from available human data since only total intestine weight was reported for monkeys.

†No urinary bladder weight was available for monkeys; equal proportions were assumed.

SUPPLEMENTAL TABLE 3. Absorbed Radiation Dose Estimates for ^{18}F-MNI-444 Using Method 1 (No Correction for Organ Weight Difference) and Method 2 (Scaled Monkey Organ Weight)

Organ	Method 1 absorbed doses (mSv/MBq)			Method 2 absorbed doses (mSv/MBq)		
	Male rhesus	Female rhesus	Mean ± SD	Male rhesus	Female rhesus	Mean ± SD
Adrenals	1.47E-02	1.91E-02	1.69E-02 ± 3.11E-03	1.37E-02	1.81E-02	1.59E-02 ± 3.11E-03
Brain	3.88E-03	8.10E-03	5.99E-03 ± 2.98E-03	4.60E-03	1.02E-02	7.40E-03 ± 3.96E-03
Breasts	7.37E-03	9.63E-03	8.50E-03 ± 1.60E-03	7.14E-03	9.45E-03	8.30E-03 ± 1.63E-03
Gallbladder wall	1.23E-01	2.74E-01	**1.99E-01 ± 1.07E-01**	1.15E-01	2.63E-01	**1.89E-01 ± 1.05E-01**
Lower LI wall	4.87E-02	4.25E-02	4.56E-02 ± 4.38E-03	2.60E-02	2.47E-02	2.54E-02 ± 9.19E-04
Small intestine	1.19E-01	1.03E-01	**1.11E-01 ± 1.13E-02**	5.66E-02	5.11E-02	**5.39E-02 ± 3.89E-03**
Stomach wall	1.52E-02	1.83E-02	1.68E-02 ± 2.19E-03	1.21E-02	1.56E-02	1.39E-02 ± 2.47E-03
Upper LI wall	1.34E-01	1.12E-01	**1.23E-01 ± 1.56E-02**	6.37E-02	5.65E-02	**6.01E-02 ± 5.09E-03**
Heart wall	1.64E-02	1.87E-02	1.76E-02 ± 1.63E-03	3.03E-02	3.24E-02	3.14E-02 ± 1.48E-03
Kidneys	2.38E-02	3.39E-02	2.89E-02 ± 7.14E-03	2.24E-02	3.34E-02	2.79E-02 ± 7.78E-03
Liver	5.35E-02	6.58E-02	**5.97E-02 ± 8.70E-03**	5.42E-02	6.73E-02	**6.08E-02 ± 9.26E-03**
Lungs	1.14E-02	1.99E-02	1.57E-02 ± 6.01E-03	1.62E-02	3.08E-02	2.35E-02 ± 1.03E-02
Muscle	1.09E-02	1.31E-02	1.20E-02 ± 1.56E-03	9.19E-03	1.15E-02	1.03E-02 ± 1.63E-03
Ovaries	2.85E-02	2.88E-02	2.87E-02 ± 2.12E-04	1.77E-02	1.92E-02	1.85E-02 ± 1.06E-03
Pancreas	1.64E-02	2.10E-02	1.87E-02 ± 3.25E-03	1.45E-02	1.93E-02	1.69E-02 ± 3.39E-03
Red marrow	1.49E-02	1.77E-02	1.63E-02 ± 1.98E-03	1.18E-02	1.47E-02	1.33E-02 ± 2.05E-03
Osteogenic cells	1.53E-02	2.11E-02	1.82E-02 ± 4.10E-03	1.34E-02	1.87E-02	1.61E-02 ± 3.75E-03
Skin	7.18E-03	8.87E-03	8.03E-03 ± 1.20E-03	6.35E-03	8.05E-03	7.20E-03 ± 1.20E-03
Spleen	1.14E-02	1.47E-02	1.31E-02 ± 2.33E-03	9.87E-03	1.33E-02	1.16E-02 ± 2.43E-03
Testes	9.20E-03	–	9.20E-03	8.12E-03	–	8.12E-03
Thymus	8.69E-03	1.15E-02	1.01E-02 ± 1.99E-03	8.68E-03	1.15E-02	1.01E-02 ± 1.99E-03
Thyroid	7.81E-03	9.54E-03	8.68E-03 ± 1.22E-03	7.30E-03	8.99E-03	8.15E-03 ± 1.20E-03
Urinary bladder wall	6.67E-02	7.28E-02	**6.98E-02 ± 4.31E-03**	6.36E-02	7.00E-02	**6.68E-02 ± 4.53E-03**
Uterus	2.55E-02	2.61E-02	2.58E-02 ± 4.24E-04	1.75E-02	1.89E-02	1.82E-02 ± 9.90E-04
Total body	1.36E-02	1.61E-02	1.49E-02 ± 1.77E-03	1.13E-02	1.42E-02	1.28E-02 ± 2.05E-03
Effective dose (mSv/MBq)	0.0275	0.0292	**0.0284 ± 0.0012**	0.0203	0.0234	**0.0219 ± 0.00219**

LI = large intestine.